

# UC Berkeley

## SEMM Reports Series

### Title

Phase Velocities of Axisymmetric Waves in Composite Rods when the Wave Length is Short

### Permalink

<https://escholarship.org/uc/item/8fm7h047>

### Authors

Mengi, Yalcin

McNiven, Hugh

### Publication Date

1967

Structures and Materials Research  
Department of Civil Engineering  
Division of Structural Engineering

Report No. 67-1

PHASE VELOCITIES OF AXISYMMETRIC  
WAVES IN COMPOSITE RODS WHEN  
THE WAVE LENGTH IS SHORT

by

Y. Mengi

Research Assistant  
University of California  
Berkeley, California, 94720

and

H.D. McNiven  
Professor of Civil Engineering  
University of California  
Berkeley, California, 94720

Structural Engineering Laboratory  
University of California  
Berkeley, California, 94720

January 1967

## SUMMARY

In this study it is found that all axisymmetric waves travelling in very long composite rods do so at the speed of certain classical waves, as the wave length approaches zero. The velocities are those of Rayleigh waves in the casing, Stoneley waves and the shear velocities in each of the core and casing materials. The number and nature of waves that exist asymptotically depend on the properties of the rod. It is found that all composite, elastic rods can be divided into four Classes and that in each Class there is a different combination of the asymptotic classical phase velocities.

## I. INTRODUCTION

1

In a previous paper<sup>1</sup>, a frequency equation was developed which governs the relationship between frequency and propagation constant for axisymmetric waves travelling in infinitely long composite rods. A pair of roots of this equation represents a propagation constant and one of its resonant frequencies. In the same paper, the frequency equation was explored for a large range of frequencies but from necessity a limited range of propagation constants, or wavelengths. These roots were shown in the form of spectral lines and it was noted how the properties of a rod influences the shape of its spectral lines. As the coordinates of a point on a spectral line are a measure of the phase velocity of waves travelling in a rod, interest was directed to how the properties of a rod influence its dispersive properties. Consideration was given to the possibility of being able to choose a rod whose properties are such that its fundamental spectral line is straight so that the rod is essentially non-dispersive. For such a design the behavior of the fundamental spectral line would have to be explored for large propagation constant which was outside the range of the previous paper.

The present paper presents the results of the study prompted by the earlier paper. In this paper, it is found that all spectral lines approach certain few straight lines asymptotically, as the propagation constant becomes infinite. As these lines emanate from the origin, each one represents a particular phase velocity. There are four possible patterns that the spectral lines can take corresponding to four types of rods. If we use the definition that the acoustically denser of two materials is the one in which the shear velocity is slower, the four rods fall into two classes; the first where the core is acoustically denser and the second

the casing. Each class of rod can be further subdivided into those rods which are capable of propagating Stoneley waves at the interface of the two materials and those that are not.

The first type of rod has a dense core and sustains Stoneley waves. For this type, the lowest or fundamental spectral line approaches the line representing the Stoneley velocity, the second and all higher approach the velocity of shear waves in the core.

The second type is the same but does not transmit Stoneley waves so that all spectral lines are asymptotic to the line representing the shear velocity of the core.

The casing of the third type of rod is denser and it can transmit Stoneley waves. Here the fundamental line and the second spectral line have as their asymptotes lines corresponding to the velocity of Rayleigh waves in the casing, and the Stoneley velocity respectively. The third and all higher branches approach the velocity of shear waves in the casing.

The fourth type is the same as the third except Stoneley waves are not possible, so that the lowest spectral line is asymptotic to the Rayleigh velocity in the casing, the second and all higher branches to the shear velocity in the casing.

As we predict that the Rayleigh, Stoneley or shear are the asymptotic velocities, it is well to try to validate this prediction using displacement distributions along a radial line of the rod. The shear velocity does not have a radial displacement distribution with which it can be characterized but the Rayleigh and Stoneley velocities do. Accordingly three points are chosen for a large propagation constant; one on the lowest spectral line for rod one and one on each of the first and second spectral lines for rod three. The displacement distributions are found and in each of the three cases the distribution has the classical form it should.

The composite rod is referred to a cylindrical coordinate system within which the radius of the core is "a" and the outer radius of the casing is "b". The two materials are bonded at their interface. The core is identified as material one and its properties are identified by a subscript one preceding the material symbol. The casing is material two. In this system,  $\rho$  represents the mass density of the core and  $v_2$  the shear velocity in the casing, etc.

The frequency equation, which was developed in a previous paper<sup>1</sup>, relates the normalized frequency  $\Omega$  and the dimensionless propagation constant  $\zeta$ , and for convenience will be repeated here. It is

$$|C_{ij}| = 0, \quad (i, j \text{ 1-6}), \quad (1)$$

where the i indicates the row and j the column. The elements of the determinant can be written.

$$\begin{aligned} C_{11} &= {}_2\alpha \lambda_1 Z_1 (\delta_2 \alpha) & C_{21} &= \zeta Z_0 (\delta_2 \alpha) \\ C_{12} &= {}_2\alpha W_1 (\delta_2 \alpha) & C_{22} &= \zeta W_0 (\delta_2 \alpha) \\ C_{13} &= -\zeta Z_1 (\delta_2 \beta) & C_{23} &= {}_2\beta Z_0 (\delta_2 \beta) \\ C_{14} &= -\zeta W_1 (\delta_2 \beta) & C_{24} &= {}_2\beta \lambda_2 W_0 (\delta_2 \beta) \\ C_{15} &= {}_1\alpha \lambda_3 Z_1 (\delta_1 \alpha) & C_{25} &= \zeta Z_0 (\delta_1 \alpha) \\ C_{16} &= -\zeta Z_1 (\delta_1 \beta) & C_{26} &= {}_1\beta Z_0 (\delta_1 \beta) \end{aligned}$$

$$\begin{aligned} C_{31} &= \mu^* [\delta (2\zeta^2 - \Omega^2) Z_0 (\delta_2 \alpha) + {}_2\alpha \lambda_1 Z_1 (\delta_2 \alpha)] \\ C_{32} &= \mu^* [\delta (2\zeta^2 - \Omega^2) W_0 (\delta_2 \alpha) + {}_2\alpha W_1 (\delta_2 \alpha)] \\ C_{33} &= 2\mu^* \zeta [\delta_2 \beta Z_0 (\delta_2 \beta) - Z_1 (\delta_2 \beta)] \\ C_{34} &= 2\mu^* \zeta [\delta_2 \beta \lambda_2 W_0 (\delta_2 \beta) - W_1 (\delta_2 \beta)] \\ C_{35} &= [\delta (2\zeta^2 - \Omega^2 v_2^{*2}) Z_0 (\delta_1 \alpha) + {}_2\alpha \lambda_3 Z_1 (\delta_1 \alpha)] \\ C_{36} &= 2\zeta [\delta_1 \beta Z_0 (\delta_1 \beta) - Z_1 (\delta_1 \beta)] \end{aligned}$$

$$\begin{aligned}
C_{41} &= -2\mu^* \zeta_2 \alpha \lambda_1 z_1 (\delta_2 \alpha) \\
C_{42} &= -2\mu^* \zeta_2 \alpha w_1 (\delta_2 \alpha) \\
C_{43} &= \mu^* (2\zeta_2^2 - \Omega^2) z_1 (\delta_2 \beta) \\
C_{44} &= \mu^* (2\zeta_2^2 - \Omega^2) w_1 (\delta_2 \beta) \\
C_{45} &= -2\zeta_2 \alpha \lambda_3 z_1 (\delta_1 \alpha) \\
C_{46} &= (2\zeta_2^2 - \Omega^2 v_2^{*2}) z_1 (\delta_1 \beta)
\end{aligned}$$

$$\begin{aligned}
C_{51} &= \delta a^* (2\zeta_2^2 - \Omega^2) z_0 (\delta_2 \alpha a^*) + 2\zeta_2 \alpha \lambda_1 z_1 (\delta_2 \alpha a^*) \\
C_{52} &= \delta a^* (2\zeta_2^2 - \Omega^2) w_0 (\delta_2 \alpha a^*) + 2\zeta_2 \alpha w_1 (\delta_2 \alpha a^*) \\
C_{53} &= 2\zeta_2 [\delta_2 \beta a^* z_0 (\delta_2 \beta a^*) - z_1 (\delta_2 \beta a^*)] \\
C_{54} &= 2\zeta_2 [\delta_2 \beta a^* \lambda_2 w_0 (\delta_2 \beta a^*) - w_1 (\delta_2 \beta a^*)] \\
C_{55} &= 0 \\
C_{56} &= 0
\end{aligned} \tag{2}$$

$$\begin{aligned}
C_{61} &= -2\zeta_2 \alpha \lambda_1 z_1 (\delta_2 \alpha a^*) \\
C_{62} &= -2\zeta_2 \alpha w_1 (\delta_2 \alpha a^*) \\
C_{63} &= (2\zeta_2^2 - \Omega^2) z_1 (\delta_2 \beta a^*) \\
C_{64} &= (2\zeta_2^2 - \Omega^2) w_1 (\delta_2 \beta a^*) \\
C_{65} &= 0 \\
C_{66} &= 0
\end{aligned}$$

The notation for each of the elements in Eqs. (2) is given in reference 1 .

Roots  $(\Omega, \zeta)$  of the frequency equation when plotted on the  $\Omega - \zeta$  plane form spectral lines which represent resonant motions of the rod.

The phase velocity is:

$$v = \frac{\Omega}{\zeta} \cdot v_2 \quad (3)$$

so  $v = \text{constant}$  is represented on the spectral plane by straight lines emanating from the origin.

The nature of the equation depends on whether the arguments of the Bessel functions are real or pure imaginary; that is whether  ${}_1\alpha, {}_2\alpha, {}_1\beta, {}_2\beta$ , are real or imaginary. It follows that there are five zones on the  $\Omega - \zeta$  plane separated by the lines

$$\begin{aligned} {}_1\alpha &= 0 \\ {}_2\alpha &= 0 \\ {}_1\beta &= 0 \\ {}_2\beta &= 0 \end{aligned} \quad (4)$$

such that the spectral lines in any one zone are derived from one of the five different frequency equations all represented by Eq. (1). The zones are pie shaped segments of the  $\Omega - \zeta$  quadrant, numbered so that zone 1 is adjacent to the  $\zeta$  axis and zone 5 adjacent to the  $\Omega$  axis. As the asymptotic phase velocities lie only in zones 1 and 2 we will restrict our attention to these two zones (see Figs 1a & 1b), and accordingly to two forms of the frequency equation. We next divide all composite rods into two classes, so that Class I contains all rods for which the core is the acoustically denser material ( $v_2^* > 1$ ) and Class II for which the casing is ( $v_2^* < 1$ ). For rods in Class I, zone 1 is separated from zone 2 by



the line

$${}_1\beta = 0 \quad (5)$$

which represents the velocity  ${}_1v_2$ . For Class II, the line

$${}_2\beta = 0 \quad (6)$$

separates the two zones, which is the line  $V = {}_2V_2$ .

We are primarily concerned in this paper with how the spectral lines behave when the wave length is very short or when the propagation constant  $\zeta$  is large. The two forms of the frequency equation are complicated, but insight into the behavior of the spectral lines is gained when we take advantage of the size of  $\zeta$ . When  $\zeta$  is large, the arguments of the Bessel functions are large, so that we can replace the Bessel functions by simpler expressions. These approximations are:

$$\begin{aligned} J_n(x) &= \left(\frac{2}{\pi x}\right)^{\frac{1}{2}} \cos\left(x - \frac{\pi}{4} - \frac{n\pi}{2}\right) \\ Y_n(x) &= \left(\frac{2}{\pi x}\right)^{\frac{1}{2}} \sin\left(x - \frac{\pi}{4} - \frac{n\pi}{2}\right) \\ I_n(x) &= (2\pi x)^{-\frac{1}{2}} e^x \\ K_n(x) &= \left(\frac{\pi}{2x}\right)^{\frac{1}{2}} e^{-x}. \end{aligned} \quad (7)$$

We will deal with each of the two forms of the frequency equation separately.

#### Zone 1

${}_1\alpha$ ,  ${}_2\alpha$ ,  ${}_1\beta$  and  ${}_2\beta$  are all imaginary in zone 1 so that the frequency equation contains only Modified Bessel functions. Using the last two of Eqs. (7) and retaining only terms of the highest order of  $\zeta$ , we find that the determinantal frequency equation breaks into the product of subdeterminants

$$\text{Exp} \left[ \mathcal{D}(a^* - 1) ({}_2\alpha + {}_2\beta) \right] D_1 D_2 = 0. \quad (8)$$

In Eq. (8)

$$D_1 = \begin{vmatrix} \left[ \delta_{a^*}(2\zeta^2 - \Omega^2) - 2_2\alpha \right] & 2\zeta(\delta_2\beta_{a^*-1}) \\ 2\zeta_2\alpha & (2\zeta^2 - \Omega^2) \end{vmatrix} \quad (9)$$

and

$$D_2 = \begin{vmatrix} 2\alpha & -\zeta & -\alpha & -\zeta \\ \zeta & -2\beta & \zeta & \beta \\ \mu^*[\delta(2\zeta^2 - \Omega^2) + 2_2\alpha] & -2\mu^*\zeta(\delta_2\beta + 1) & [\delta(2\zeta^2 - \Omega^2 v_2^{*2}) - 2_2\alpha] & 2\zeta(\delta_2\beta - 1) \\ -2\mu^*\zeta_2\alpha & \mu^*(2\zeta^2 - \Omega^2) & 2\zeta_1\alpha & [2\zeta^2 - \Omega^2 v_2^{*2}] \end{vmatrix} \quad (10)$$

When  $D_1$  is expanded and a term of a lower order of  $\zeta$  is dropped it becomes the equation

$$(2\zeta^2 - \Omega^2)^2 = 4\zeta_2^2 \alpha_2 \beta, \quad (11)$$

which we recognize as the equation governing the Rayleigh wave velocity.

The second determinant is more easily recognized in the form:

$$D_2 = \begin{vmatrix} \left(1 - \frac{s^2}{2k^2}\right)^{\frac{1}{2}} & -1 & -\left(1 - \frac{v_2^{*2}}{k^2} s^2\right)^{\frac{1}{2}} & -1 \\ 1 & -(1-s^2)^{\frac{1}{2}} & 1 & (1-v_2^{*2} s^2)^{\frac{1}{2}} \\ \mu^*(2-s^2) & -2\mu^*(1-s^2)^{\frac{1}{2}} & (2-v_2^{*2} s^2) & 2(1-v_2^{*2} s^2)^{\frac{1}{2}} \\ -2\mu^*\left(1 - \frac{s^2}{2k^2}\right)^{\frac{1}{2}} & \mu^*(2-s^2) & 2\left(1 - \frac{v_2^{*2}}{k^2} s^2\right)^{\frac{1}{2}} & (2-v_2^{*2} s^2) \end{vmatrix} \quad (12)$$

which is the equation developed by Stoneley<sup>2</sup> governing the phase velocity of Rayleigh-type waves travelling along a bonded interface of two materials.

If we denote this velocity as  $V_{st}$ , we have

$$S = V_{st} / v_2$$

It would be advisable here to review Stoneley waves and what has been found about the equation

$$D_2 = 0. \quad (13)$$

At an interface of two materials, Stoneley waves may or may not exist,<sup>2</sup> that is there may not be a real "s" which satisfies Eq. (12). Sezewa and Kanai<sup>3</sup> have shown that in general a real root "s" exists only when the shear velocities in each of the two materials are close to one another or when  $V_2^*$  does not differ greatly from one. When Stoneley waves do exist, their velocity is a constant so that the waves are non-dispersive. This can be understood when we note that  $D_2$  is independent of the frequency or propagation constant. Koppe<sup>4</sup> established that the lower bound of  $V_{st}$  is the Rayleigh velocity of the acoustically dense medium and also found that the displacements will decrease exponentially into each of the two materials away from the interface (the assumption of Stoneley) so long as the Stoneley wave velocity is less than the shear velocity of the acoustically dense material.

In zone one, therefore, only Rayleigh and Stoneley velocities are possible when  $\zeta$  is large.

#### Zone 2

In zone 2 we will examine in detail Class I rods.  ${}_1\alpha$ ,  ${}_2\alpha$ ,  ${}_2\beta$  are pure imaginary,  ${}_1\beta$  is real in zone 2, Class I. Using Eqs. (7) the frequency equation for zone 2 takes the form

$$D_3 = 0 \quad (14)$$

where



where

$$\begin{aligned}
 m_1 &= \frac{\sqrt{\beta}}{\zeta} = (1-s^2)^{\frac{1}{2}} & n_1 &= \frac{\sqrt{\alpha}}{\zeta} = \left(1 - \frac{s^2}{2k^2}\right)^{\frac{1}{2}} \\
 m_2 &= \frac{\sqrt{\beta}}{\zeta} = (v_2^* 2s^2 - 1)^{\frac{1}{2}} & n_2 &= \frac{\sqrt{\alpha}}{\zeta} = \left(1 - \frac{v_2^{*2}}{k^2} s^2\right)^{\frac{1}{2}}
 \end{aligned} \tag{17}$$

With some further manipulation Eq. (16) can be put in the form

$$\tan \left( \delta \cdot m_2 - \frac{3\pi}{4} \right) = \frac{\Delta_A}{\Delta_B} \tag{18}$$

where

$$\Delta_A = \begin{vmatrix} 1 & m_1 & 1 \\ \mu^{*(1+m_1^2)-2} & 2m_1(\mu^*-1) & -(1+m_2^2) \\ n_1 \left[ (1-m_2^2) - 2\mu^* \right] & \left[ (1-m_2^2) - \mu^{*(1+m_1^2)} \right] & n_2 (1+m_2^2) \end{vmatrix} \tag{19}$$

$$\Delta_B = m_2 \begin{vmatrix} n_1 & 1 & -n_2 \\ \mu^{*(1+m_1^2)-2} & 2m_1(\mu^*-1) & -(1+m_2^2) \\ n_1 \left[ (1-m_2^2) - 2\mu^* \right] & \left[ (1-m_2^2) - \mu^{*(1+m_1^2)} \right] & n_2 (1+m_2^2) \end{vmatrix} \tag{20}$$

The behavior of the spectral lines in zone 2, when  $\zeta$  is large, is contained in Eq. (18) which is sufficiently simple for qualitative analysis. The behavior will become apparent when we can find the roots "s" for a particular, large  $\zeta$ , say  $\bar{\zeta}$ . On the left side of the equation, "s" appears only in the  $m_2$  of the argument  $(\delta \bar{\zeta} \cdot m_2 - \frac{3\pi}{4})$ . We now examine the plot of  $\tan \left( \delta \bar{\zeta} \cdot m_2 - \frac{3\pi}{4} \right)$  in Fig. (2) and establish the bounds of its argument as fixed by the bounds of zone 2. The lower bound of zone 2 is the line  $\sqrt{\beta} = 0$  which gives

$$m_2 = 0. \tag{21}$$

This establishes the lower bound of the angle  $(\delta \bar{\zeta} \cdot m_2 - \frac{3\pi}{4})$  as  $(-\frac{3\pi}{4})$ .

The upper bound of zone 2 can either be the line  $\alpha = 0$  or  $\beta = 0$  but, as each of the lines is straight, "s" is a constant and therefore  $m_2$  is a constant say  $\bar{m}_2$ . This means that for a particular rod in Class I the upper bound of the angle is  $(\delta \bar{\zeta} \bar{m}_2 - \frac{3\pi}{4})$ .  $\tan(\delta \bar{\zeta} \bar{m}_2 - \frac{3\pi}{4})$  is then sketched over the extent of this interval as "s" varies over the extent of zone 2.

We next examine the right side of Eq. (18) and note that

$$\frac{\Delta A}{\Delta B} = \frac{\Delta A}{\Delta B} (s, \mu^*, \rho^*, \nu_1, \nu_2),$$

so for a given rod the right side is a function of "s" only and further that as "s" approaches the lower bound,  $m_2$  approaches zero and the function goes to infinity. So for a particular  $\bar{\zeta}$  the sketch shown in Fig. (2) is a probable plot of both sides of Eq. (18) so that points of intersection give the roots "s". Regardless of whether  $\Delta A / \Delta B$  approaches plus infinity or minus infinity, the lowest intersection occurs very close to  $(-\pi/2)$ . If we set

$$(\delta \zeta m_2 - \frac{3\pi}{4}) = -\frac{\pi}{2} \tag{22}$$

we find that the lowest velocity is

$$s_1 = \frac{1}{v_2^*} \left( 1 + \frac{\pi^2}{16 \delta^2 \zeta^2} \right)^{\frac{1}{2}} \tag{23}$$

As  $\zeta$  becomes large, "s" approaches  $\frac{1}{v_2^*}$  from above or the phase velocity V approaches  $v_2$  from above. So the lowest spectral line in zone 2 approaches the lower bound of zone 2 asymptotically.

In Fig. (2) the second intersection is close to, say  $(\frac{\pi}{4})$  and if we set the argument of the angle equal to  $(\frac{\pi}{4})$  we find the second velocity,

$$s_2 = \frac{1}{v_2^*} \left(1 + \frac{\pi^2}{\delta^2 \zeta^2}\right)^{\frac{1}{2}} \quad (24)$$

so we can conclude that the second spectral line in zone 2 approaches the same asymptote as the first, as  $\zeta$  goes to infinity, but approaches it more slowly.

The number of roots for a particular  $\bar{\zeta}$  represents the number of spectral lines in zone 2 that intersect the line  $\zeta = \bar{\zeta}$ . If we take a new line say  $\zeta = 2\bar{\zeta}$  we find that the interval of the angle  $(\delta\zeta m_2 - \frac{3\pi}{4})$  within zone 2 almost doubles because the left boundary remains the same but the right boundary moves to the right almost twice as far from the origin as it was before. Consequently there will be almost twice the roots "s" at  $\zeta = 2\bar{\zeta}$  as there were for  $\zeta = \bar{\zeta}$ . The additional spectral lines have entered zone 2 from zone 3. If we use the arguments just set forth, we can make the general statement that all spectral lines, except the lowest one or two, enter zone 2 and eventually approach its lower bound if the propagation constant becomes sufficiently large.

Though the same qualitative analysis for Class II rods was not made, numerical analysis of a few rods in this class, using the full frequency equation, leads us to conclude that the spectral lines in Class II have the same pattern as in Class I.

### III. THE FOUR TYPES OF RODS

There are four different patterns that the spectral lines can take as  $\zeta$  becomes large, and these will be demonstrated by examining the spectral line for four different rods. Two rods are in each of the two Classes and in each Class one rod will be capable of propagating Stoneley waves and one

will not. The properties of the four rods are listed in Table 1.

Table 1

	$\mu^*$	$\rho^*$	$a^*$	${}_1V$	${}_2V$
Rod 1	.204	.10	1.5	.25	.25
Rod 2	4.0	2.0	2.0	.25	.25
Rod 3	4.902	10.0	2.0	.25	.25
Rod 4	.1075	.2914	8.0	.29	.20

Rod 1 (Fig. 3)

This rod is in Class I and it transmits Stoneley waves. The lowest asymptotic phase velocity for this rod is the Stoneley velocity. The only velocity which could be less would be that of Rayleigh waves in the core material but these are not possible. Here the lowest spectral line is asymptotic to the straight line for which  $V = V_{st}$ , and all of higher spectral lines have as their asymptote the straight line represented by  $V = {}_1V_2$ . As Rayleigh waves can travel along the casing, resonance will always occur along the line  $V = {}_2V_R$  which is accommodated by means of the terracing observed in the figure.

Rod 2 (Fig. 4)

This rod is also in Class I but, as no Stoneley waves exist, all of the spectral lines, including the lowest will have the line  $V = {}_1V_2$  as their asymptote. The terracing for Rayleigh waves in the casing is the same as for rod 1.

Rod 3 (Fig. 5)

This rod is in Class II, with Stoneley waves. Here the lowest velocity is that of Rayleigh waves in the casing and is represented by the line  $V = {}_2V_R$ . The lowest spectral line is asymptotic to this line, the second is asymptotic to  $V = V_{st}$  and the third and all higher spectral lines are asymptotic to the line  $V = {}_2V_2$ . As Rayleigh waves are not possible



in the core there is no terracing.

Rod 4 (Fig. 6)

Class II with no Stoneley waves, so the lowest spectral line is asymptotic to the line  $V = {}_2V_R$  and the second and all higher spectral lines are asymptotic to the line  $V = {}_2V_2$ .

#### IV. DISPLACEMENT DISTRIBUTIONS

We have predicted that, for certain rods, trains of waves associated with the lowest spectral lines travel at the speed of Rayleigh and Stoneley waves when the wave length is short. It is important therefore to explore whether displacement distributions, along radial lines, conform to the patterns associated with these types of waves.

Accordingly we derive expressions for the magnitude of the displacement components valid for any combination of frequency and propagation constant.

If we include only the radial dependency, the components are:

$${}_1u_r = A_1 \left[ \frac{A_5}{A_1} {}_1\alpha \lambda_3 Z_1({}_1\alpha \delta R) - \frac{A_6}{A_1} \zeta Z_1({}_1\beta \delta R) \right]$$

$${}_2u_r = A_1 \left[ -{}_2\alpha \lambda_1 Z_1({}_2\alpha \delta R) - \frac{A_2}{A_1} {}_2\alpha W_1({}_2\alpha \delta R) \right. \\ \left. + \frac{A_3}{A_1} \zeta Z_1({}_2\beta \delta R) + \frac{A_4}{A_1} \zeta W_1({}_2\beta \delta R) \right]$$

$${}_1u_z = A_1 \left[ \frac{A_5}{A_1} \zeta Z_0({}_1\alpha \delta R) + \frac{A_6}{A_1} {}_1\beta Z_0({}_1\beta \delta R) \right]$$

$${}_2u_z = -A_1 \left[ \zeta Z_0({}_2\alpha \delta R) + \frac{A_2}{A_1} \zeta W_0({}_2\alpha \delta R) \right. \\ \left. + \frac{A_3}{A_1} {}_2\beta Z_0({}_2\beta \delta R) + \frac{A_4}{A_1} {}_2\beta \lambda_2 W_0({}_2\beta \delta R) \right]$$

The  $\lambda$ 's, Z's and W's are defined in Ref. (1),  $R = \frac{r}{a}$  and the  $\frac{A_i}{A_1}$  ( $i=2\dots6$ ) are found from any five of the six boundary conditions expressed as Eqs. (16) Reference 1

The distributions have been found for three combinations of frequency and propagation constant. The first combination identifies a point on the lowest spectral line for Rod 1 (see point 1 Fig. 3) for which the phase velocity is the Stoneley velocity. The radial and axial displacement distributions corresponding to this point, which are shown in Fig. (7), indeed show the Stoneley wave distribution. As was pointed out in Reference 1. the radial and axial components of displacement act ninety degrees out of phase.

Points two and three (see Fig. 5) are on the lowest two spectral lines of Rod 3 which predict Rayleigh and Stoneley phase velocities respectively. The displacement distributions for these two points are shown in Figures (8) and (9). Point two shows the Rayleigh wave distribution and point three the Stoneley wave distribution, as they should.

#### ACKNOWLEDGEMENT

The authors wish to acknowledge that the research was supported by the National Science Foundation through a Research Grant to the University of California at Berkeley.

CAPTIONS FOR FIGURES

- Fig. 1a The Spectral Zones for Class I Composite Rods
- Fig. 1b The Spectral Zones for Class II Composite Rods
- Fig. 2 Graphical Solution of the Reduced Frequency Equation for Class I Rods in Zone 2
- Fig. 3 Spectrum for Rod 1 Showing Frequency VS Real Propagation Constant
- Fig. 4 Spectrum for Rod 2 Showing Frequency VS Real Propagation Constant
- Fig. 5 Spectrum for Rod 3 Showing Frequency VS Real Propagation Constant
- Fig. 6 Spectrum for Rod 4 Showing Frequency VS Real Propagation Constant
- Fig. 7 The Radial and Axial Displacement Distributions Corresponding to the Point 1, for Rod 1
- Fig. 8 The Radial and Axial Displacement Distributions Corresponding to the Point 2, for Rod 3
- Fig. 9 The Radial and Axial Displacement Distributions Corresponding to the Point 3, for Rod 3

REFERENCES

- 1 H.D. McNiven, J.L. Sackman, and A.H. Shah, "Dispersion of Axially Symmetric Waves in Composite, Elastic Rods," The Journal of the Acoustical Society of America, Vol. 35, No. 10, 1602-1609, October, 1963.
- 2 Stoneley, R., "Elastic Waves at the Surface of Separation of Two Solids", Proc. Roy. Soc. (London), A, Vol. 106, pp. 416-428, 1924.
- 3 Sezewa, K., and K. Kanai, "The Range of Possible Existence of Stoneley Waves and Some Related Problems", Bull Earthquake Research Institute (Tokyo), Vol. 17, pp. 1-8, 1939.
- 4 Koppe, H., "Über Rayleigh-Wellen an der Oberfläche Zweier Medien," Z. Angew. Math. U. Mech., Vol. 28, pp. 355-360, 1948.

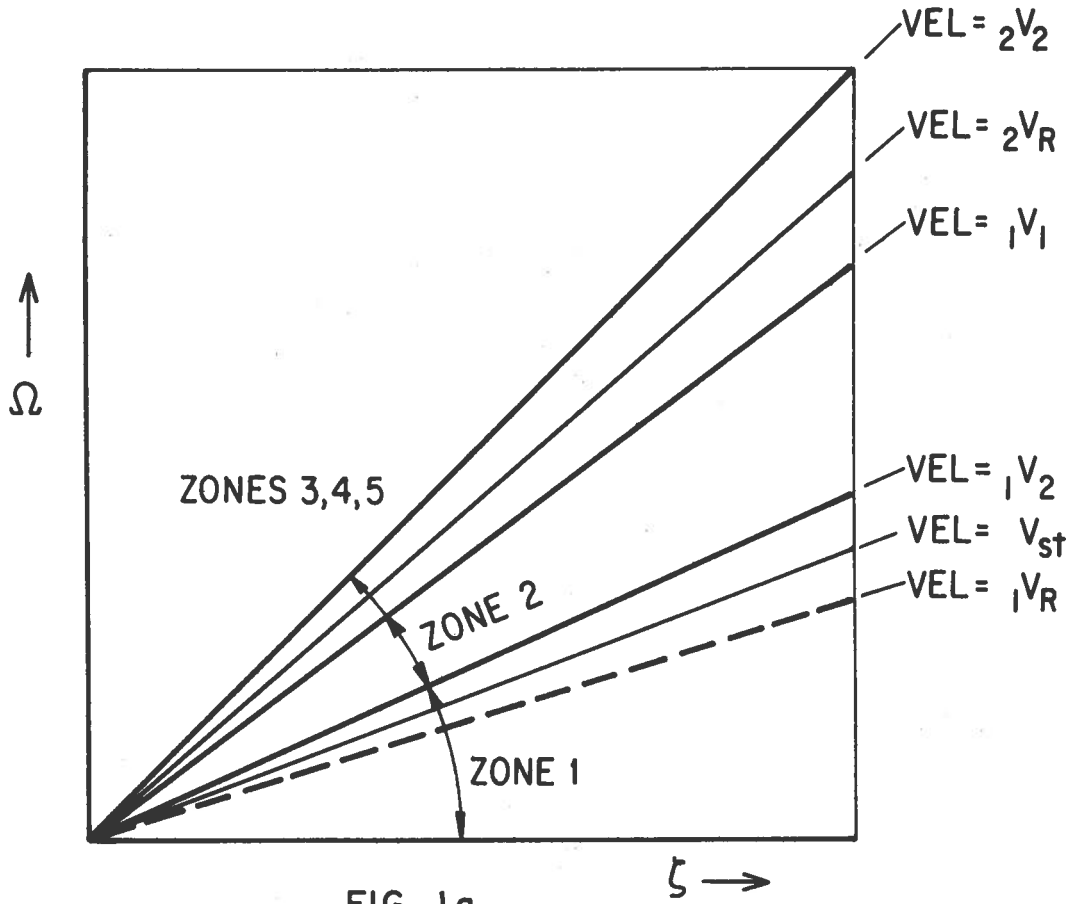


FIG. 1a

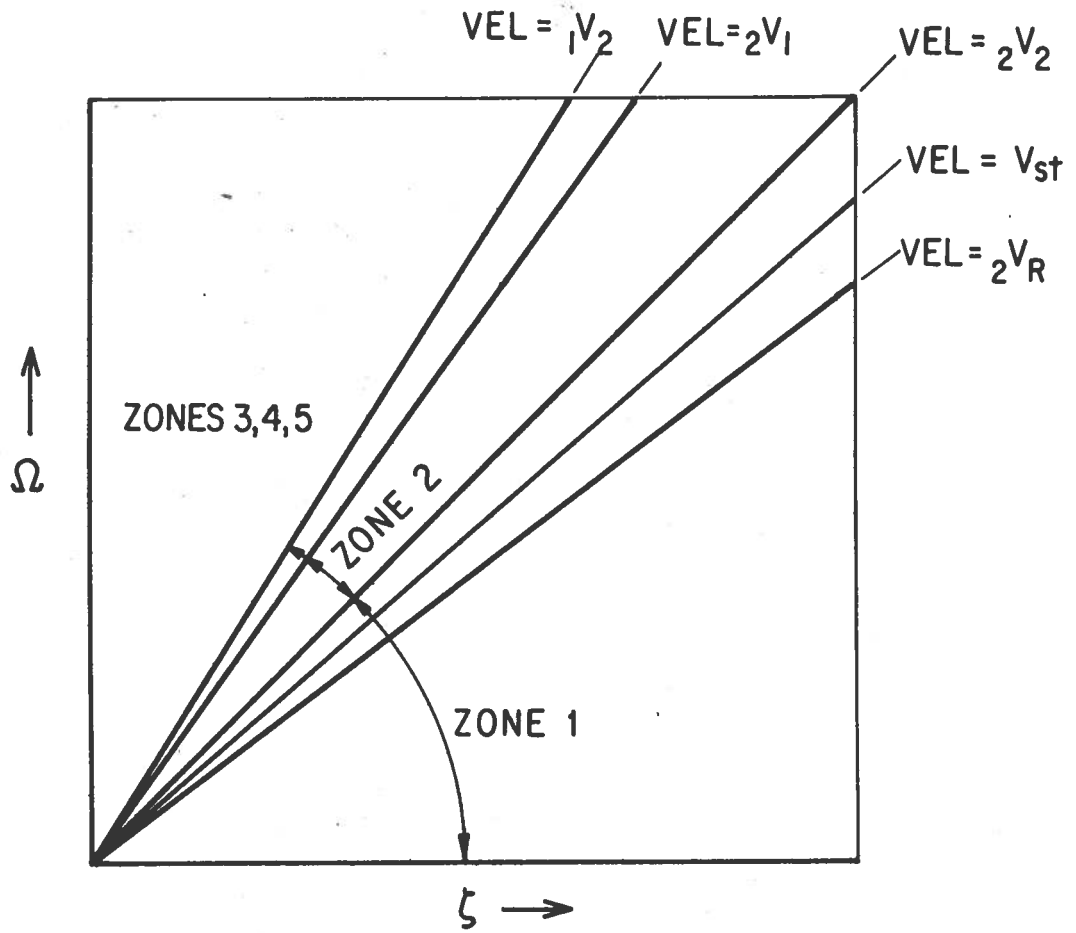


FIG. 1b

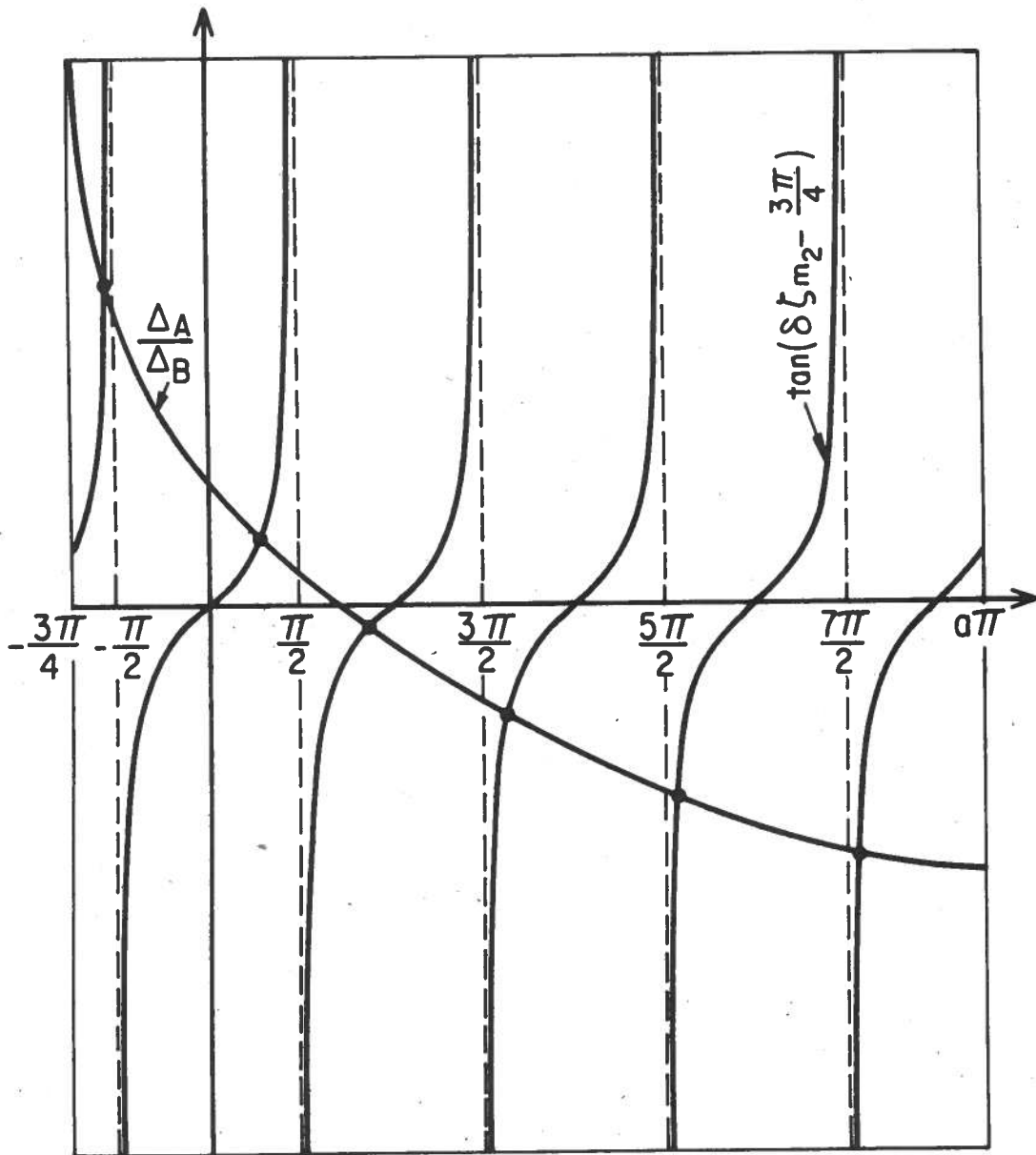


FIG. 2

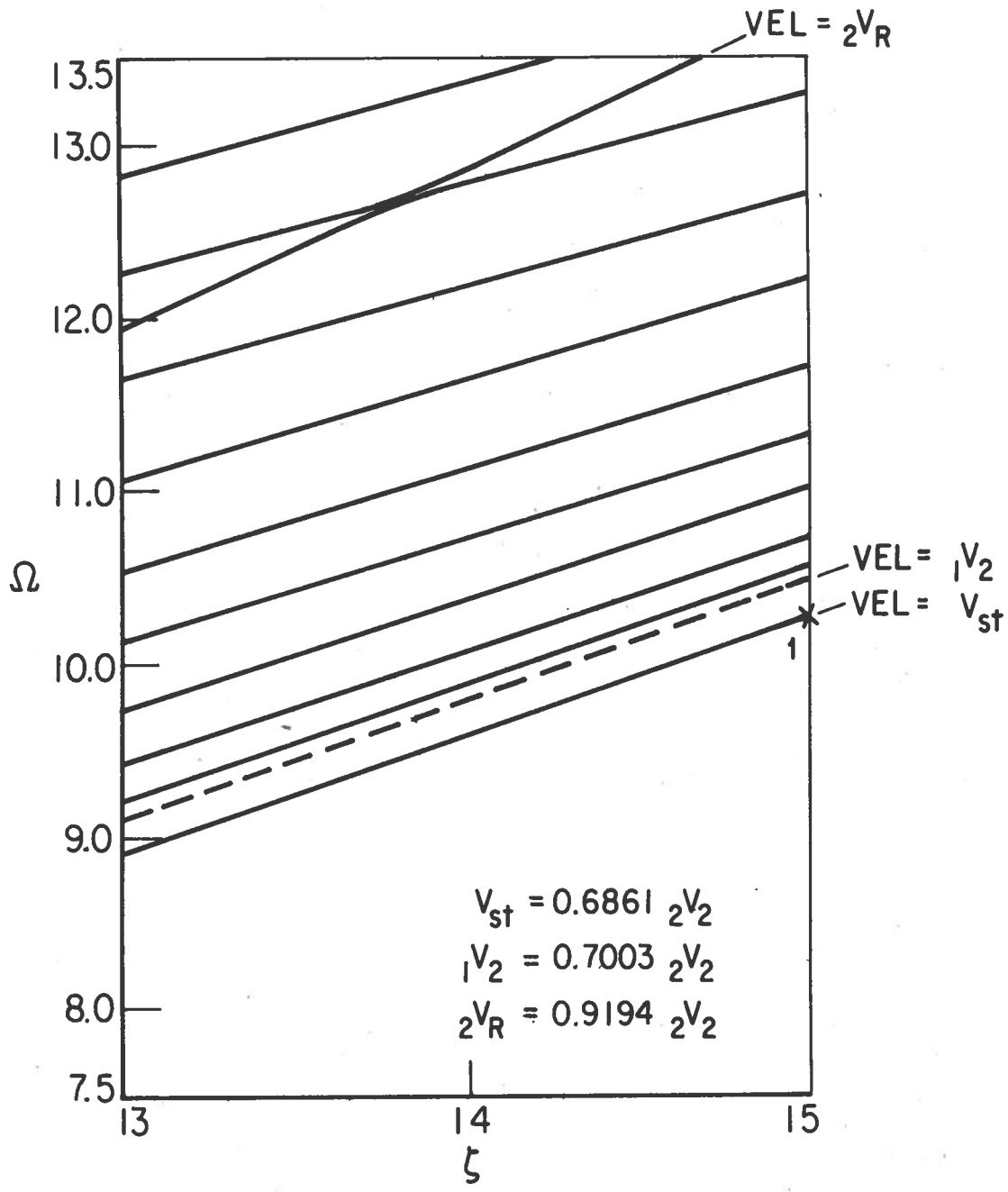


FIG. 3

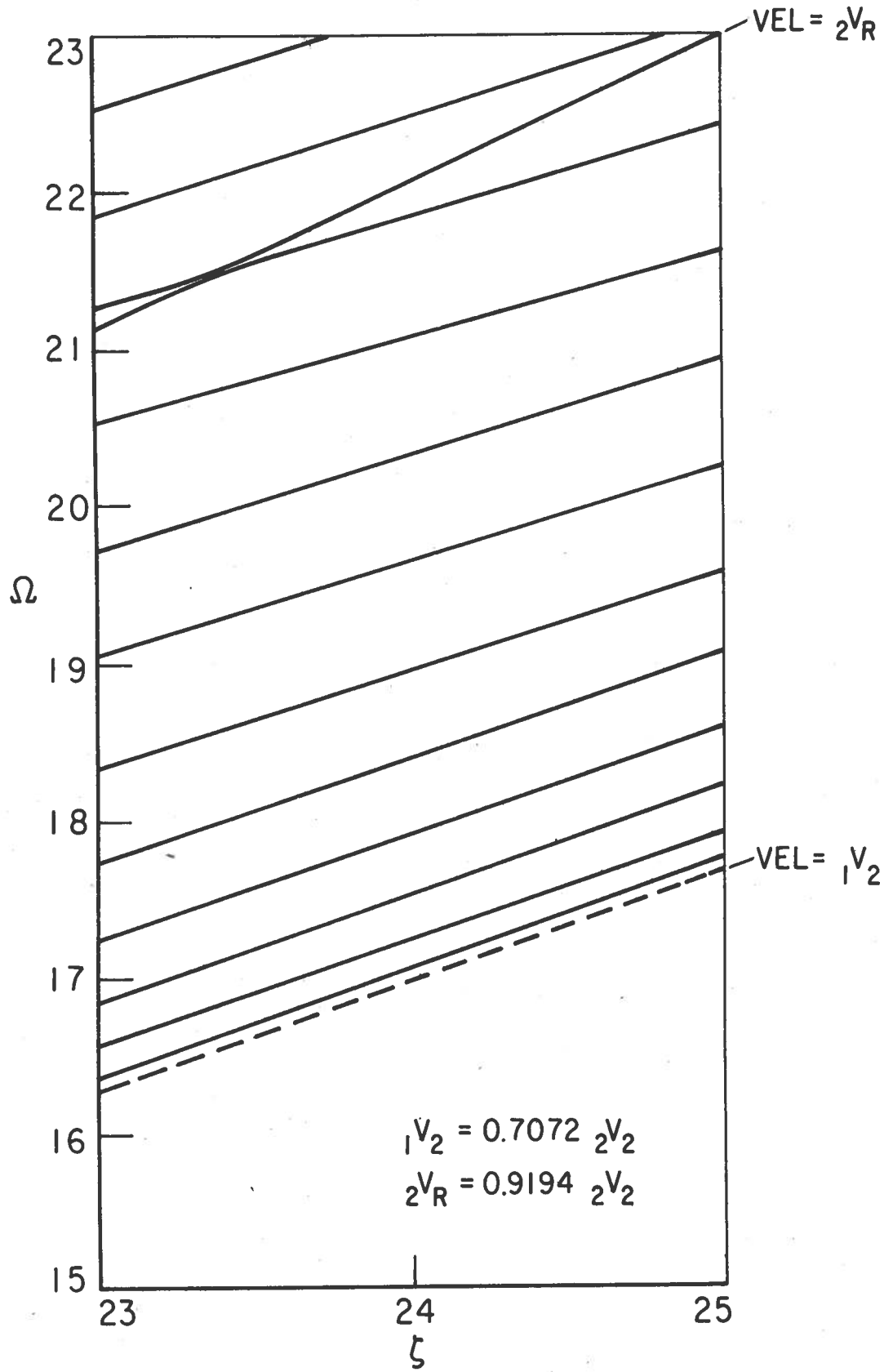


FIG. 4



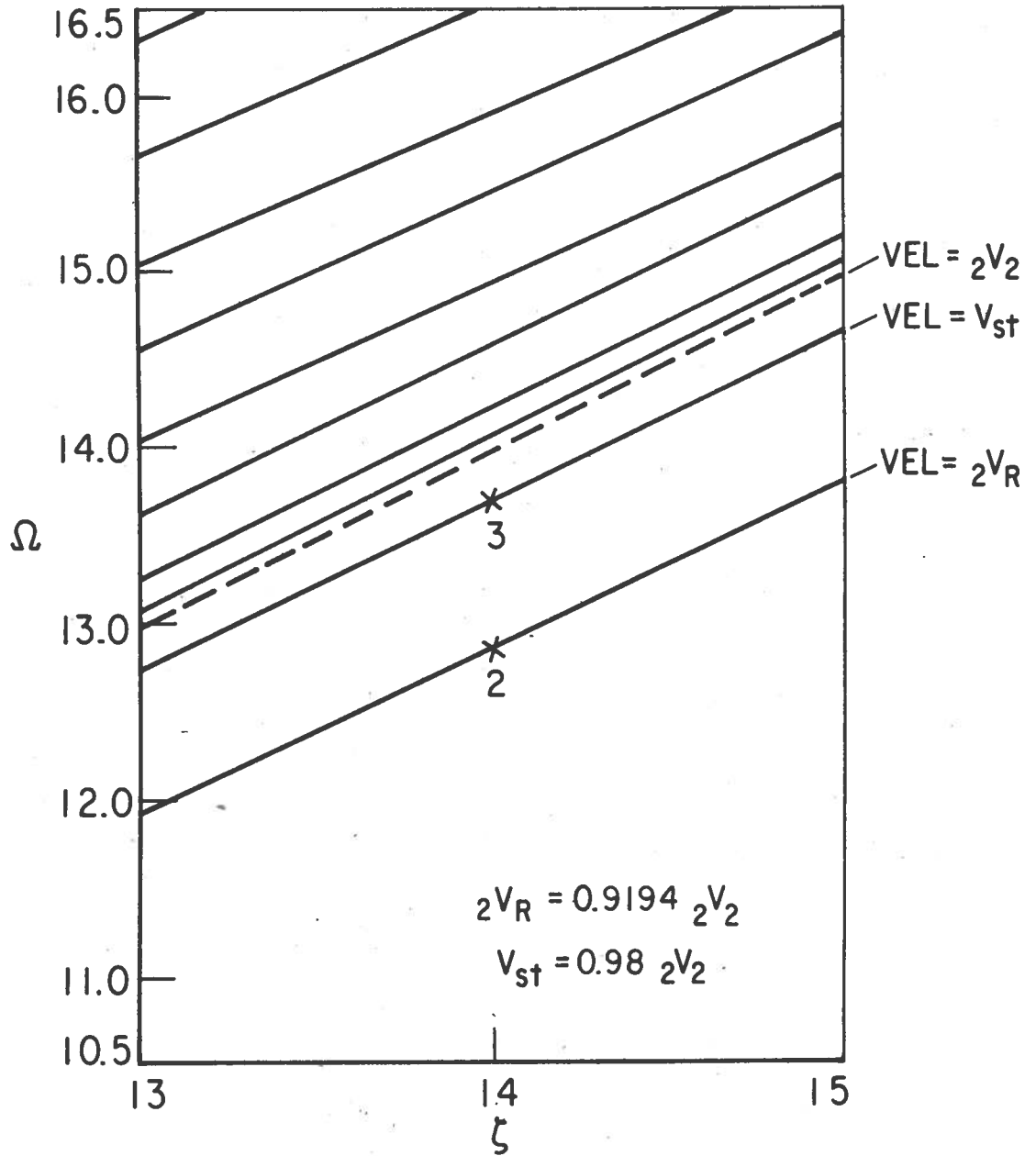


FIG. 5

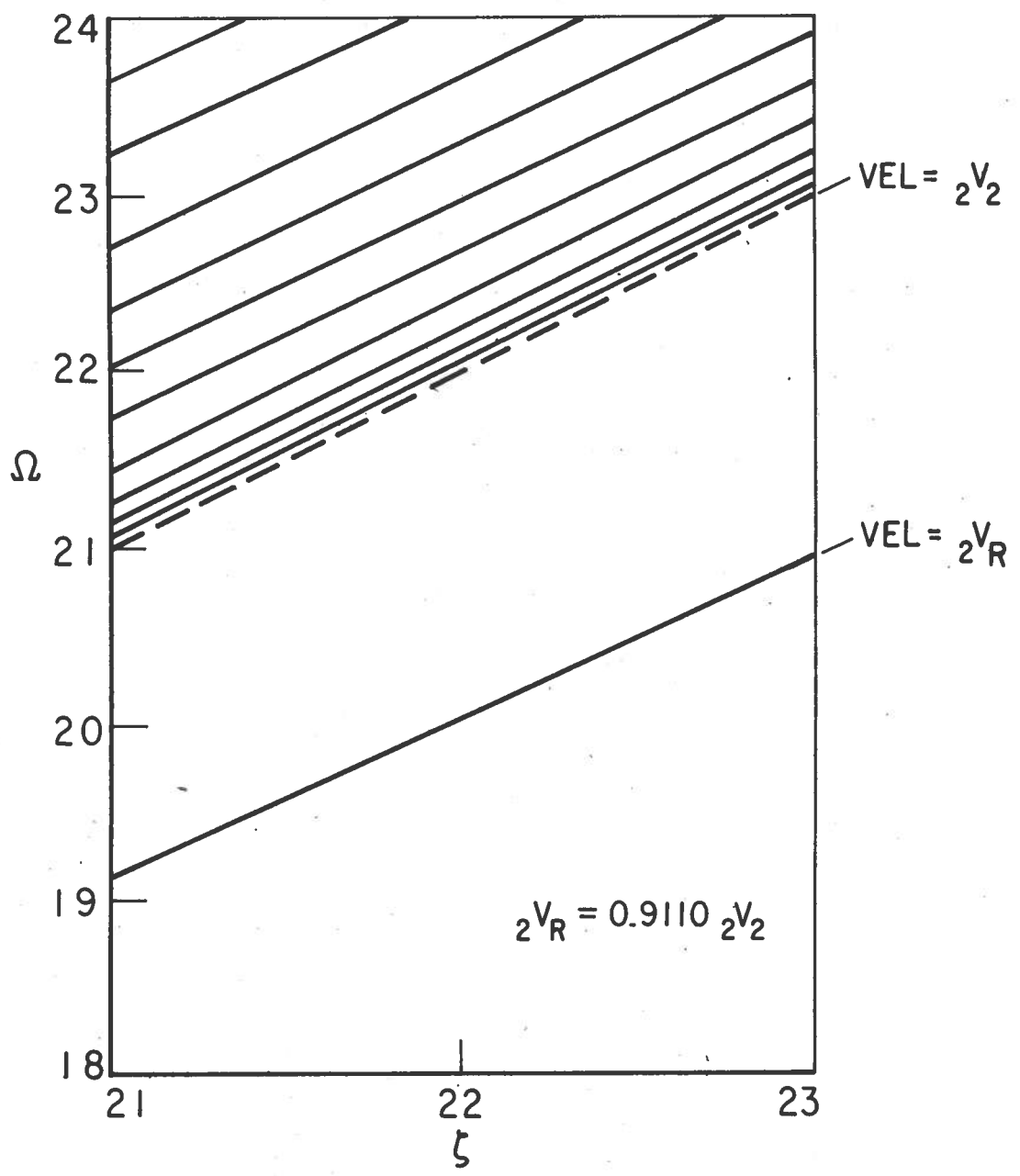


FIG. 6

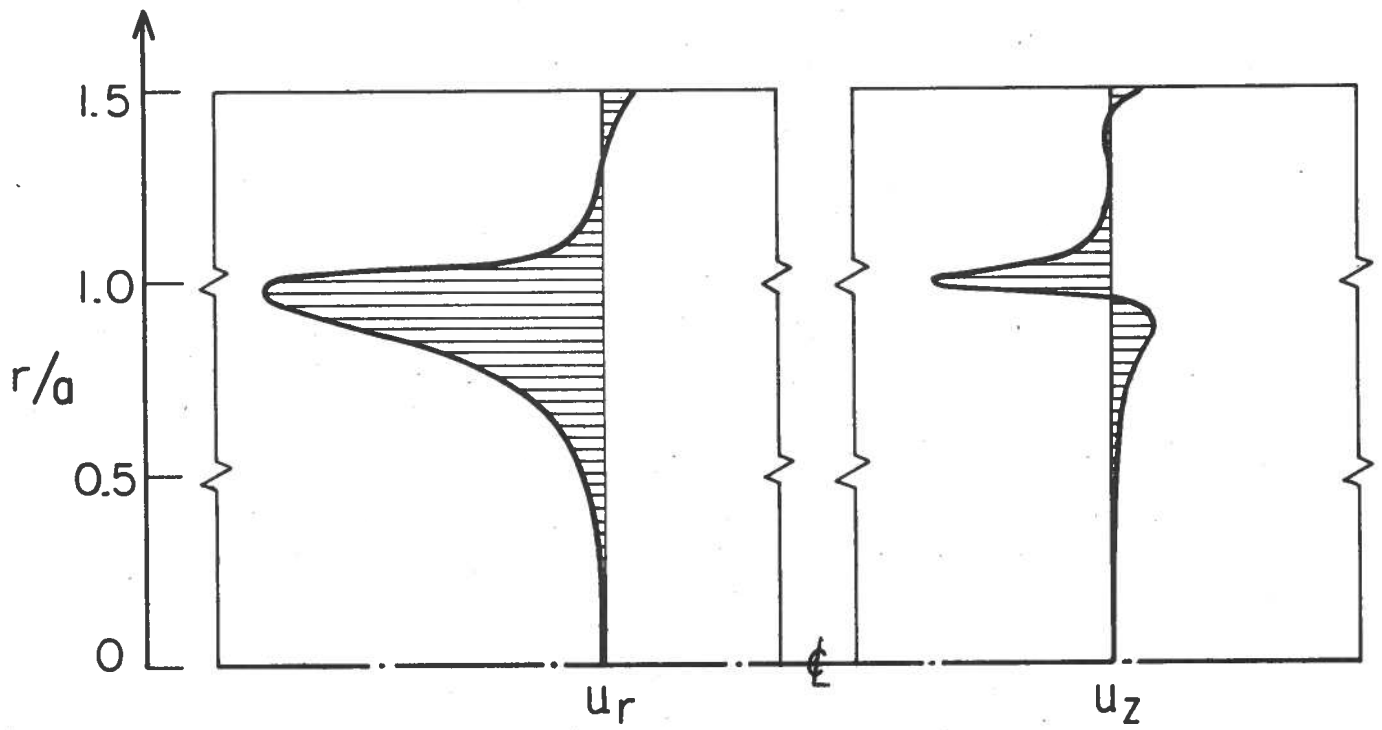


FIG. 7

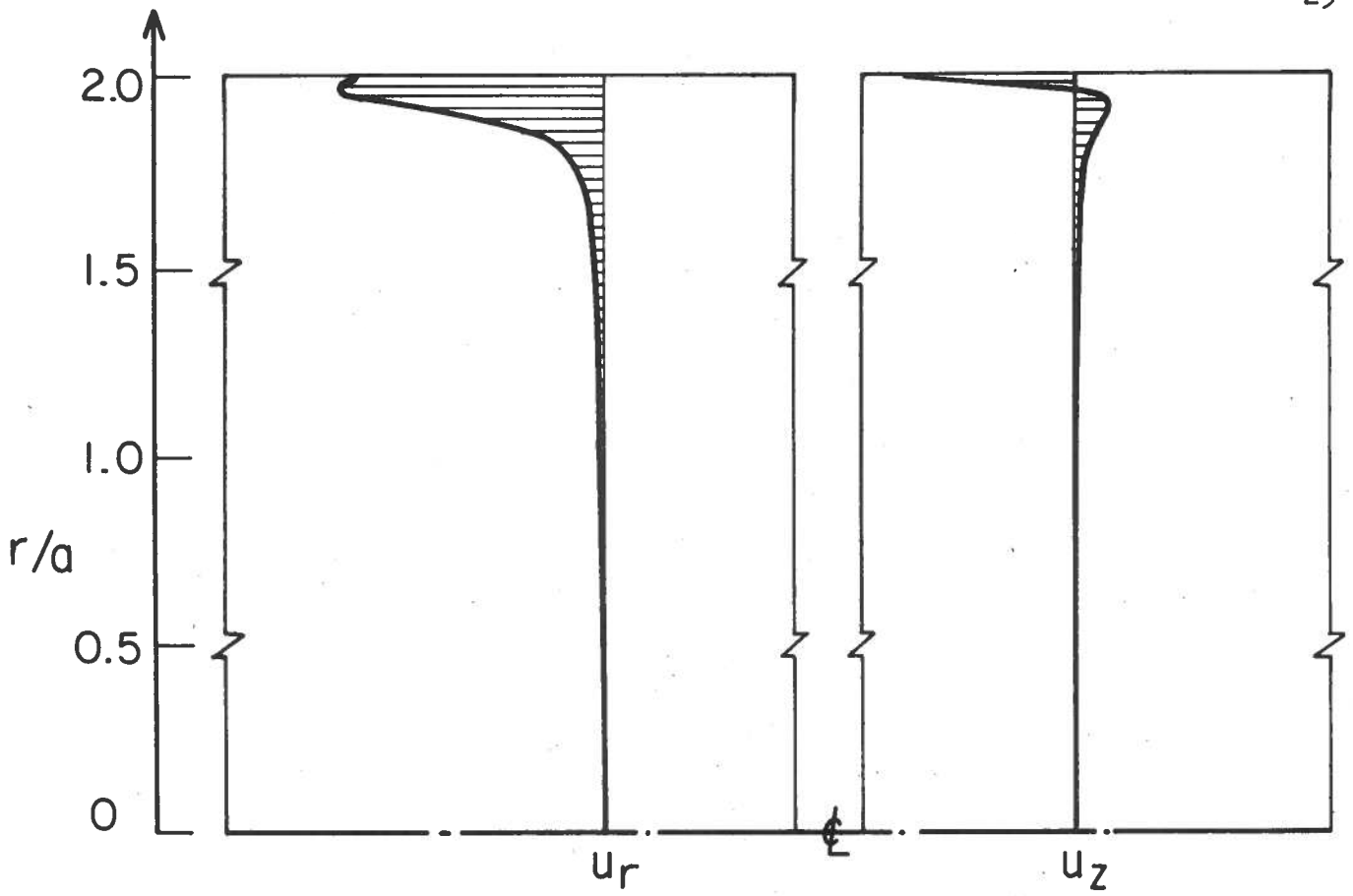


FIG. 8

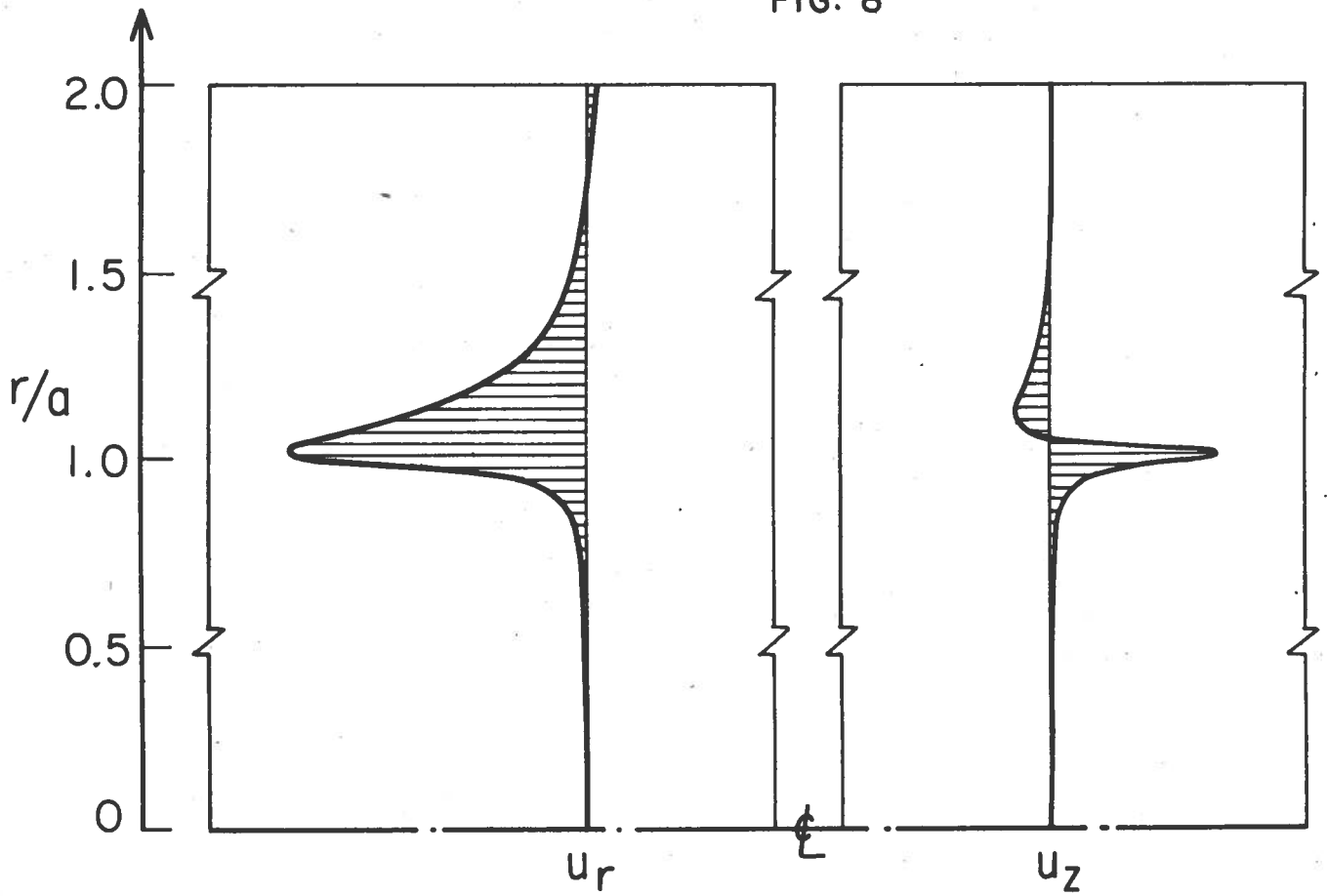


FIG. 9